

# Experimental Electron Density Distribution and QTAIM Topological Analysis for the Perovskite Mineral: Sulphohalite – Na<sub>6</sub>(SO<sub>4</sub>)<sub>2</sub>FCl

Agata Wróbel, dr Roman Gajda, prof. dr hab. Krzysztof Woźniak.  
Department of Chemistry, Biological and Chemical Research Centre, University of Warsaw, Poland

## Outline

The acquaintance of *modern crystallography onto mineralogy* will be approached by endeavouring in an experimental charge density study for the double antiperovskite mineral – sulphohalite [Na<sub>6</sub>(SO<sub>4</sub>)<sub>2</sub>FCl]. *High-resolution* X-ray diffraction data was collected employing *AgKα* radiation ( $\lambda = 0.56087 \text{ \AA}$ ) to a resolution of **0.3941 Å** at **100K**. The crystal structure was solved by direct methods implementation based on merged SHELX data – in compliance with the *Independent Atom Model (IAM)*. *Electron density (ED)* distribution –  $\rho(\mathbf{r})$  was modelled, as proposed in the Hansen-Coppens formalism, by consecutive least-square multipolar refinements. The *quality* of collected data and computed ED model was assessed; conclusively it proved to be of high grade.

## High-resolution data collection and ED refinement

Table 1. Crystal data for sulphohalite.

Crystal	Sulphohalite
Chemical Formula	Na <sub>6</sub> (SO <sub>4</sub> ) <sub>2</sub> FCl
Formula molecular mass [g/mol]	384.51
Crystal System	Cubic
Space Group	Fm $\bar{3}$ m
<i>a</i> [Å]	10.03124(7)
Volume [Å <sup>3</sup> ]	1009.40(2)
<i>Z</i>	4
<i>D<sub>x</sub></i> [g/cm <sup>3</sup> ]	2.530
$\mu$ [mm <sup>-1</sup> ]	0.552
<i>F</i> (000)	752.0
Crystal size [mm <sup>3</sup> ]	0.129 × 0.081 × 0.070

Table 2. Data collection for sulphohalite.

Data collection	Sulphohalite
Temperature [K]	100(2)
Radiation type	Ag K $\alpha$ ( $\lambda = 0.56087 \text{ \AA}$ )
2 $\theta$ range for data collection [°]	5.55 to 89.306
Diffractometer	Agilent Technologies SuperNova
Absorption correction	SCALE3 ABSPACK
<i>T<sub>min</sub></i> , <i>T<sub>max</sub></i>	0.5019, 1.0000
No. of measured, independent and observed [ <i>I</i> > 2 $\sigma$ ( <i>I</i> )] reflections	5847, 477, 477
<i>R<sub>int</sub></i> , <i>R<sub>sigma</sub></i>	0.0675, 0.0263
Index Ranges	-25 ≤ <i>h</i> ≤ 25; -25 ≤ <i>k</i> ≤ 25; -25 ≤ <i>l</i> ≤ 25
$\sin\theta/\lambda_{\text{max}}$ (Å <sup>-1</sup> )	0.500

Table 3. Refinement features for the *Independent Atom Model (IAM)* and the *Multipole Model (MM)*.

Refinement	IAM	MM
Data / restraints / parameters	477 / 0 / 10	477 / 22 / 33
Goodness-of-fit on <i>F</i> <sup>2</sup>	1.0390	2.8895
Final <i>R</i> indexes [ <i>I</i> > 2 $\sigma$ ( <i>I</i> )] on <i>F</i> <sup>2</sup>	<i>R</i> <sub>1</sub> = 0.0292; <i>wR</i> <sub>2</sub> = 0.0496	<i>R</i> <sub>1</sub> = 0.0188; <i>wR</i> <sub>2</sub> = 0.0423
Final <i>R</i> indexes [all data] on <i>F</i> <sup>2</sup>	<i>R</i> <sub>1</sub> = 0.0323; <i>wR</i> <sub>2</sub> = 0.0830	<i>R</i> <sub>1</sub> = 0.0229; <i>wR</i> <sub>2</sub> = 0.0698
Largest diff. peak/hole [e·Å <sup>-3</sup> ]	0.488 / -1.477	0.402 / -0.846

## Deformation of ED – Δρ(r)

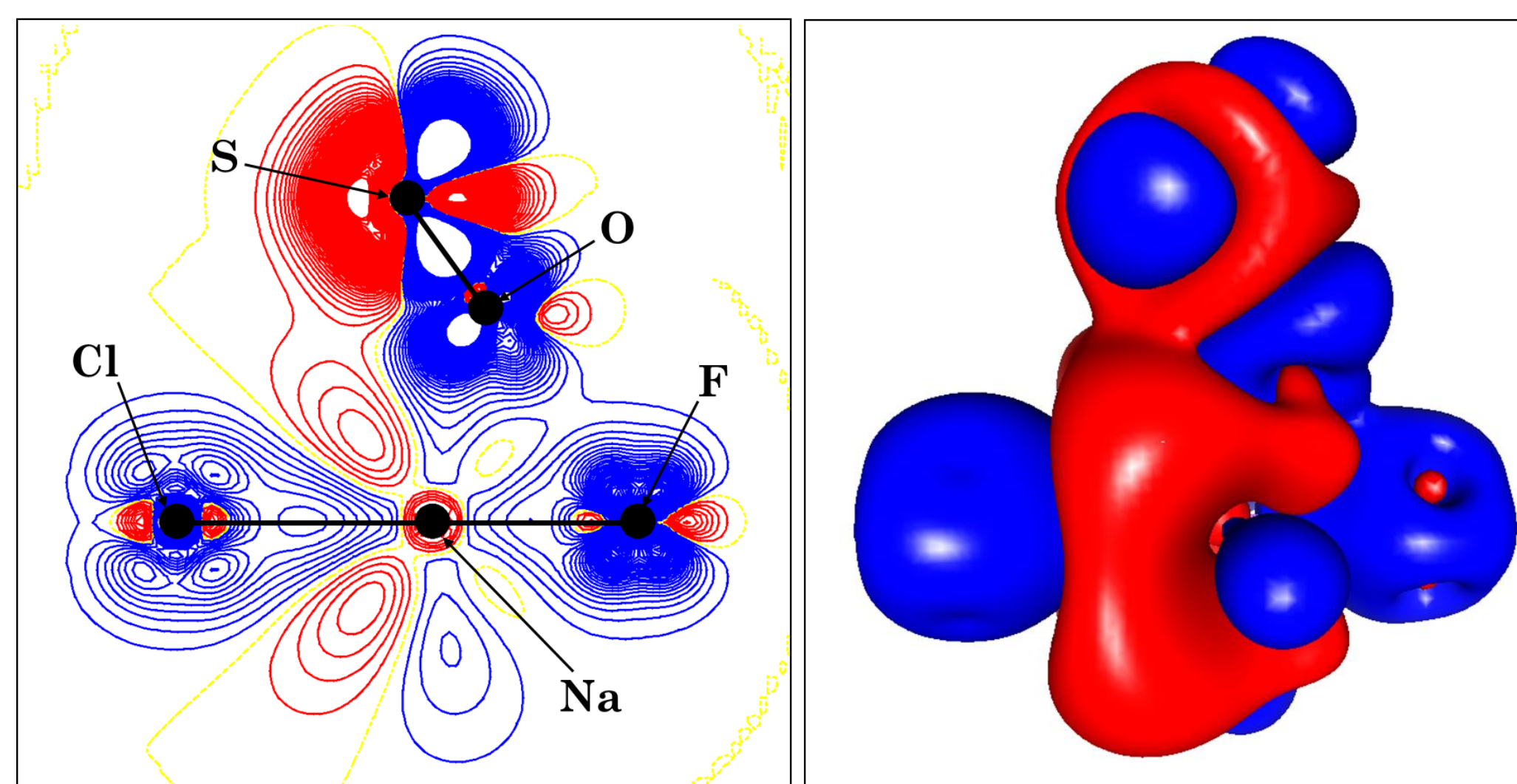


Fig 3. 2D and 3D Static Deformation of ED maps – calculated based on the subtraction of the IAM from the MM model and projected on to the (011) plane. Positive and negative values of the function are correspondingly denoted by blue and red. Standard contour levels are drawn up to  $\pm 0.001 \text{ e}\cdot\text{\AA}^{-3}$ . Zero contour lines are presented in yellow. 3D surface corresponds to the isovalue:  $\pm 0.001 \text{ e}\cdot\text{\AA}^{-3}$ .

## Atomic Basins (AB's)

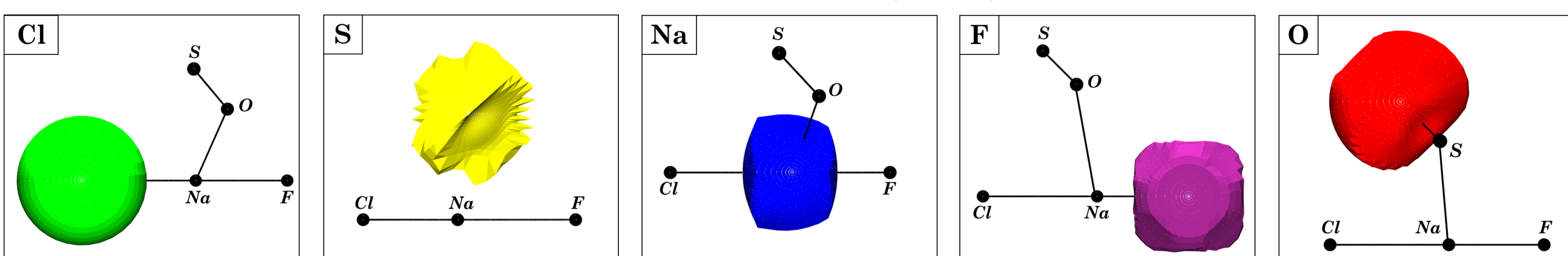


Fig 5. Atomic Basins (AB) computed for each atom in sulphohalite.

Table 7. Computed AB volumes and charges.

Atom	<i>V<sub>ab</sub></i> [Å <sup>3</sup> ]	<i>Q<sub>ab</sub></i> [e]
Cl	38.920	-0.836
S	5.656	3.168
Na	7.931	0.910
F	14.178	-1.334
O	17.416	-1.227

Table 8. Percentage of "unaccounted" unit cell volume by experimental AB.

Unit cell volume	<i>V</i> [Å <sup>3</sup> ]	<i>V</i> [%]
<i>V</i> = <i>a</i> <sup>3</sup>	1009.389	100.0
$\Sigma(n \cdot V_{ab})$	1005.293	99.594
$\Delta[V - \Sigma(n \cdot V_{ab})]$	4.095	0.406

Table 9. Percentage of "unaccounted" unit cell charge by experimental AB.

Unit cell charge	<i>n</i> [e]	<i>n</i> [%]
Number of electrons – $\Sigma(n \cdot Z)$	752.0	100.0
Number of "unaccounted" electrons – $\Sigma(n \cdot Q_{ab})$	-0.750	0.010

Table 10. Atomic Lagrangian – *L*, for computed AB in the sulphohalite crystal.

Atom	Cl	S	Na	F	O
Atomic Lagrangian - <i>L</i>	$1.401 \cdot 10^{-2}$	$1.042 \cdot 10^{-3}$	$1.726 \cdot 10^{-3}$	$1.460 \cdot 10^{-3}$	$4.899 \cdot 10^{-3}$

## Crystal structure

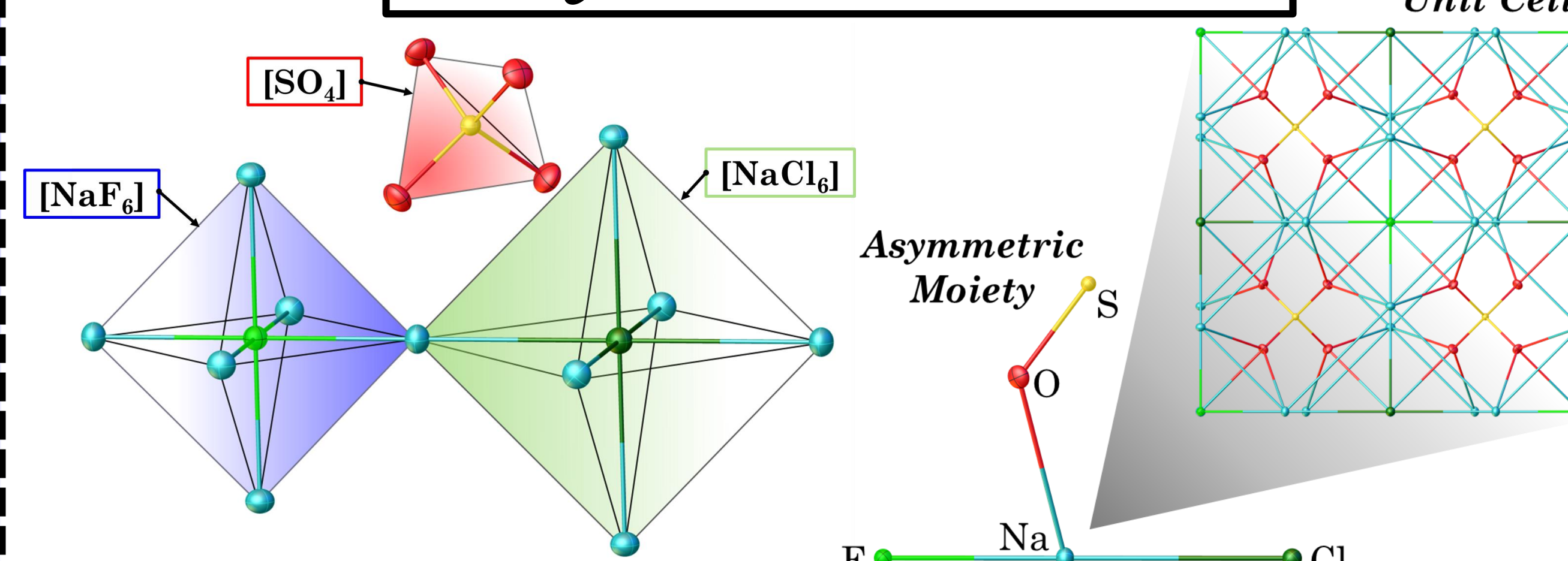


Fig 1. The crystal structure of sulphohalite is presented as a polyhedral construct. Displacement ellipsoids are drawn at a 60% probability level.

Fig 2. The asymmetric moiety and the unit cell of the sulphohalite crystal. Displacement ellipsoids are drawn at a 60% probability level.

## QTAIM – Topological Analysis

### Gradient Vector Field of ED – ∇ρ(r)

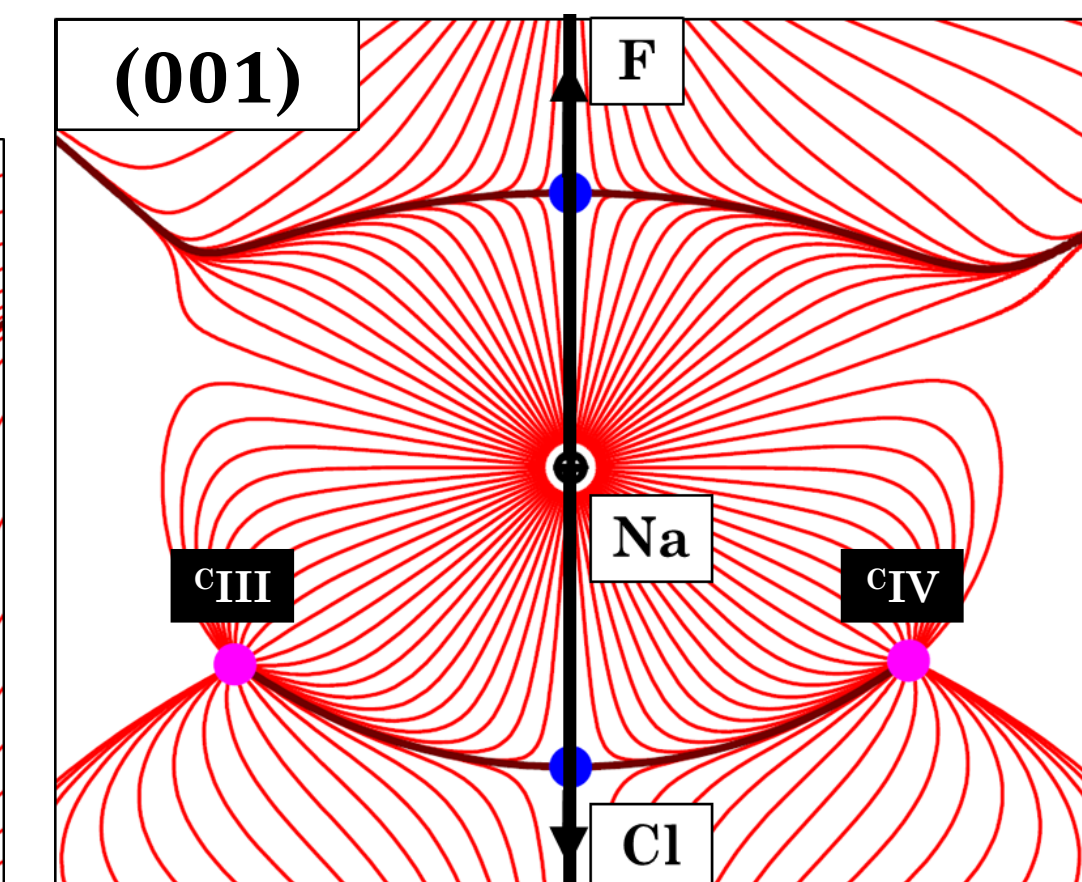
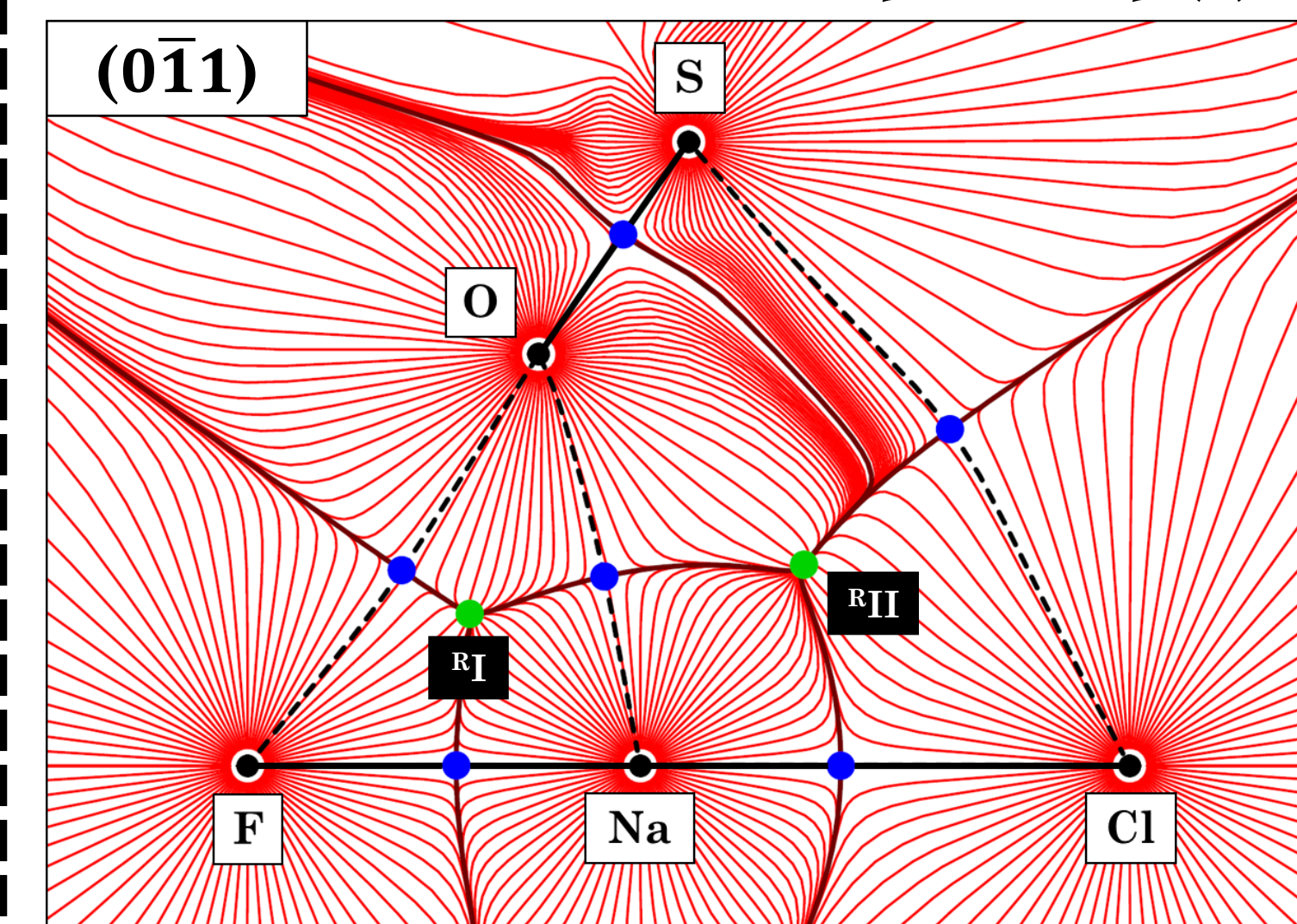


Fig 4. Gradient vector field of ED, drawn for two planes in the crystal of sulphohalite. Bond, Ring and Cage CP's are respectively denoted by blue, green, and magenta circles. Interatomic bonding is presented by black lines; whereas bonding paths are depicted by black dashed lines.

### Laplacian of ED – ∇²ρ(r)

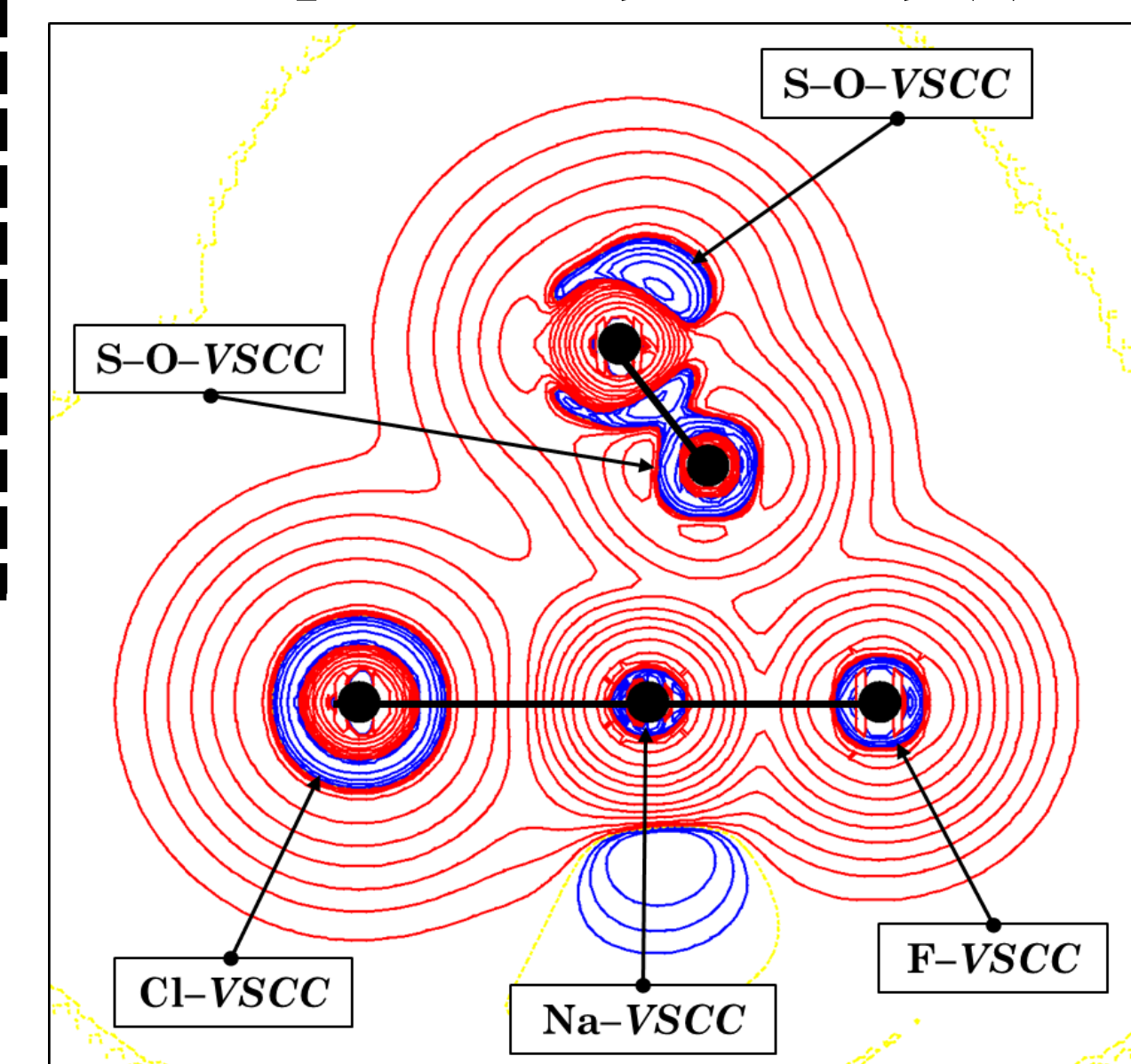


Fig 6. Valence Shell Charge Concentrations (VSCC's), denoted on the 2D Laplacian of ED contour plot drawn onto the sulphohalite's (011) plane. Logarithmic contour levels are drawn up to  $\pm 0.001 \text{ e}\cdot\text{\AA}^{-3}$ . Positive and negative values of the function are correspondingly denoted by blue and red. Zero contour lines are presented in yellow.

### Critical Points (CP's)

Table 4. Bond Critical Point (BCP) features.

BCP type	$\rho(r_{\text{BCP}})$ [e·Å <sup>-3</sup> ]	$\nabla^2\rho(r_{\text{BCP}})$ [e·Å <sup>-5</sup> ]	Ellipticity - $\epsilon$
Cl...S	0.008	0.120	0.090
Cl...Na	0.126	0.575	0.000
S-O	2.484	-31.00	0.002
Na...O	0.129	1.931	0.197
Na...F	0.207	3.022	0.000
F...O	0.061	0.868	0.340

Table 5. Ring Critical Point (RCP) features.

RCP type	$\rho(r_{\text{RCP}})$ [e·Å <sup>-3</sup> ]	$\nabla^2\rho(r_{\text{RCP}})$ [e·Å <sup>-5</sup> ]
R <sub>I</sub>	0.0520	R0.912
R <sub>II</sub>	-0.0018	0.332
R <sub>III</sub> , R <sub>IV</sub> , R <sub>V</sub>	-0.0070	0.201

Table 6. Cage Critical Point (CCP) features.

CCP type	$\rho(r_{\text{CCP}})$ [e·Å <sup>-3</sup> ]	$\nabla^2\rho(r_{\text{CCP}})$ [e·Å <sup>-5</sup> ]
C <sub>I</sub> , C <sub>II</sub>	-0.025	0.514
C <sub>III</sub> , C <sub>IV</sub>	-0.026	0.401

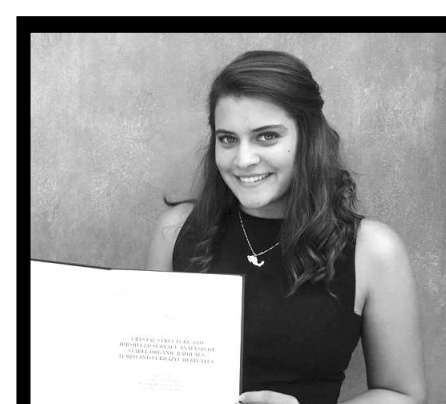
### Interatomic Interactions

Table 11. Evaluation of the nature of interatomic interactions according to the *dichotomous* classification.

Interatomic Interaction	Cl...S	Cl...Na	S-O	Na...O	Na...F	F...O
$\nabla^2\rho(r_{\text{BCP}})$ [e·Å <sup>-5</sup> ]	> 0	> 0	< 0	> 0	> 0	> 0
VSCC overlap at BP	No	No	Yes	No	No	No
Outcome	Closed-Shell	Closed-Shell	Shared-Shell	Closed-Shell	Closed-Shell	Closed-Shell

## Conclusions

Topological analysis according to the *Quantum Theory of Atoms in Molecules – QTAIM* was undertaken based on the experimentally attained distribution of charge. *Atomic basins (AB's)* were delineated based on the *zero flux surfaces (ZFS's)* denoted on the *gradient vector field of ED – ∇ρ(r)*. The appertaining volumes and charges of each basin were computed by full-volume integration. Following, *critical points (CP's)* were identified as local extrema of the  $\nabla\rho(\mathbf{r})$  function, and classified based on the *Laplacian of ED – ∇²ρ(r)*. Morse's 'characteristic set' condition was met. The study of *primary bundles (PB's)*, as proposed by Pendás, revealed the interconnection between AB's and CP's onto *basins of attraction* or *basins of repulsion*. The nature of interatomic interactions was assessed through the *dichotomous* classification. The S-O contact was acknowledged as a *covalent* with a *shared-shell*. The remaining contacts were characterized as *non-covalent* closed-shell (Cl...Na, Na...O and Na...F) or *weak van der Waals* closed-shell (Cl...S and F...O).



This research was supported by the Polish National Science Centre (NCN) (grant agreement No. UMO-2019/33/B/ST10/02671), and was carried out at the Biological and Chemical Research Centre, University of Warsaw, established within the project co-financed by European Union from the European Regional Development Fund under the Operational Programme Innovative Economy, 2007 – 2013.

